Evaluation of Digital Rock Mass Discontinuity Mapping Techniques for Applications in Tunnels

P K K Wu*, J Chin, R Tsui, C Ng

Aurecon Hong Kong Limited, Hong Kong, China

*Corresponding author

doi: https://doi.org/10.21467/proceedings.133.38

ABSTRACT

High-quality coloured 3D point clouds can now be readily generated by digital surveying techniques such as structure from motion (SfM) photogrammetry and terrestrial laser scanning (TLS). Point clouds allow discontinuities to be mapped digitally on rock slopes and this has been widely studied in Hong Kong. In comparison, few similar applications have been reported in tunnels in Hong Kong. To extend the application of this technology for tunnel excavation, we carried out three site trials in two drill-and-blast hard rock tunnels in Hong Kong. Both SfM photogrammetry and TLS were used to generate point clouds for the exposed rock tunnel surfaces. The generated point clouds were then tested for semi-automatic extraction of rock mass discontinuities using DRM2.0, Aurecon's in-house developed software. This paper provides detail accounts of data acquisition, data processing, present the findings on the performance of semi-automatic identification of discontinuities, and the comparison between SfM and TLS techniques. The paper also discusses the challenges in digital mapping inside tunnels and provide useful suggestions on conducting laser scanning and photogrammetry in tunnels.

Keywords: Photogrammetry, Laser Scanning, Digital Rock Tunnel Mapping

1 Introduction

Tunnel face mapping is a vital step in tunnel excavation process that is traditionally carried out by an engineering geologist. One of the main purposes of tunnel mapping is to determine the quality of the rock mass through observation of rock discontinuities such as orientation, spacing, persistence and roughness as part of rock mass quality parameters. The task of face mapping itself consists of two major challenges: the first being that mapping must be completed within very limited timeframe between scaling and temporary support installation; and second, when the same exposed tunnel face is mapped by different geologists, the result could potentially vary due to the degree of skill and experience of the geologist (as much as the estimation of the characteristics of rock discontinuities from some distance of the tunnel face due to the unsupported zone, underlying personal judgment, human error or bias).

Point cloud data has been widely used in the construction industry thanks to the recent rapid growth of digital surveying technology. As high-quality coloured 3D point clouds can now be readily generated, the new technology further diversified the application of point clouds. And it can now be applied to geotechnical engineering such as rock mass discontinuity mapping. Between December 2019 and March 2021, the GEO organized a benchmarking exercise on digital rock mass discontinuity survey for rock slopes, which formed part of the Innotech Forum on Geotechnology 2021 in March 2021. We were invited to this Forum and presented the findings of digital rock mass discontinuity survey.

While digital rock mass discontinuity mapping has been applied to rock slopes in Hong Kong (Gibbons et al. 2019; Wong et al. 2019; CEDD 2021), few similar studies have been conducted in tunnels in Hong Kong (e.g. Chan et al. 2019). We carried out three site trials in tunnels to extend the application of this technology for tunnel excavation. These site trials were conducted in two drill-and-blast hard rock tunnels in Hong Kong. Two remote sensing techniques, namely structure from motion (SfM) photogrammetry and terrestrial laser scanning (TLS), were used to generate point clouds for the

Proceedings DOI: 10.21467/proceedings.133; Series: AIJR Proceedings; ISSN: 2582-3922; ISBN: 978-81-957605-1-0

exposed rock tunnel surfaces. The point clouds were then tested for semi-automatic extraction of rock mass discontinuities using DRM2.0 (Aurecon's in-house developed software) and Facet.

2 Site Description

The two drill-and-blast tunnels (Tunnel A and Tunnel B) where trails were carried out are located in Hong Kong. Trial 1 and 2 were carried out in Tunnel A, while Trial 3 in Tunnel B. The tunnel faces of Trial 1 and 3 were excavated by drill and blast method while the tunnel face of Trial 2 was excavated by drill and break method. Figure 1 summarizes the excavated dimensions of the tunnel face, the tunnel depth and the rock mass characteristics at the three site trials. The rock mass characteristics were estimated by the mapping geologists and were agreed by the authors.

For Trial 1, the tunnel face is formed in strong to very strong Grade II medium-grained granite with massive rock mass. The Q' value was estimated to be 5.6. For Trial 2, the tunnel face is formed in strong to very strong Grade II/III fine-grained granite, with an estimated Q' value of 3.35. For Trial 3, the tunnel face comprises strong Grade II lapilli-bearing fine ash tuff, with an estimated Q' value of 2.89. Based on the observation on site, the rock mass overall becomes blockier from Trial 1 to Trial 3. It is also consistent with the factor of RQD / Jn which describes the degree of jointing (or block size). It should be noted that Q' differs from Q in that Q' is obtained from RQD, Jn, Jr, and Ja while Q is obtained with Jw and SRF in addition to the aforementioned four parameters.

Figure 1: Photos of the tunnel faces in Trial 1 to Trial 3, with dimensions and ground conditions at the bottom.

3 Data Acquisition and Processing

The data acquisition, including laser scanning and photo-taking, was completed within a short timeframe during the mapping and surveying time after mucking out. The data acquisition procedures require minimal additional arrangements in the tunnel except for the preparation of ground control points. Back in the office, the raw data were readily converted into point clouds by sophisticated commercial software. Details of the data acquisition and data processing are provided below.

3.1 Terrestrial Laser Scanning (TLS)

The TLS in Trial 1 to Trial 3 were carried out by a Leica BLK360 Imaging Laser Scanner. The scanner is equipped with a 15 megapixel 3-camera system for spherical imaging, therefore coloured point clouds can be produced. In the site trials, the scanner was positioned approximately 10 to 15m away from the tunnel face. To minimize occlusions (areas of lack of point cloud data, usually at the shadow of a

protruding object which cannot be captured by laser scanner / camera, e.g. a horizontal discontinuity plan facing upward and located at higher level), two laser scans were taken at different positions to generate the point cloud. The scan locations in Trial 2 are shown as an example in Figure 2.
The scanner was carefully levelled prior to scanning. In Trial 1, the scans were in taken in medium-resolution mode. In Trials 2 and 3, the scans were in taken high-resolution mode. Each scan took 4-7 minute. No spherical / black and white targets were needed.

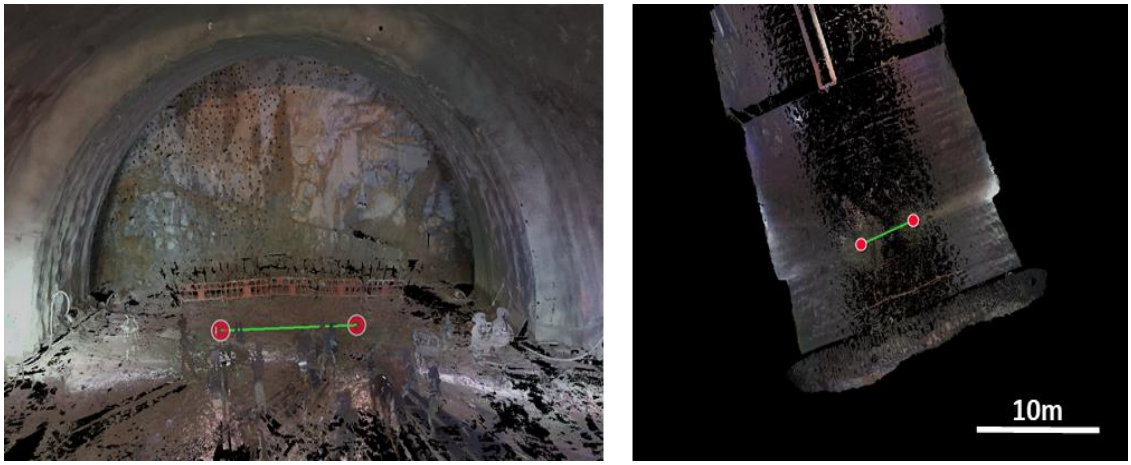

Figure 2: Laser scanner locations (red dots) in Trial 2

Back to office, the scans were registered automatically without any targets with Leica's software, Cyclone Register 360. The registration error was approximately 2 to 3mm. The resultant point clouds generated are approximately 30 to 40m in range. The subsequent data processing is discussed in Section 3.3.

3.2 Structure-from-motion (SfM) Photogrammetry

We carried out SfM and TLS simultaneously in Trials 1 and 2. The SfM technology works by extracting and matching feature points across photos, estimating the camera orientations, calculating the 3D locations of feature points, and finally constructing a dense point cloud.

In a review on using SfM technology for geomorphological research, Micheletti et al. (2015) provided a list of suggestions on taking photos for SfM technology. These include maintaining a static scene, using consistent lighting, taking photos from different positions and orientations, and avoiding different zoom settings and flashlights, among others. These suggestions are generally followed in our site trials.

In our trials, the photos were taken by a 24.2 Megapixel full-frame mirrorless camera equipped with a 24mm f/1.8 prime lens. The camera must be mounted on a tripod for stability since the exposure time was relatively long. Consistent camera settings were used throughout each trial, as summarized in Table 1.

Table 1: Camera settings used in Trial 1 and Trial 2

Trial #	Shutter speed (s)	Aperture	ISO
Trial 1	1/8	f/7.1	1000
Trial 2	1/6	f/7.1	1000

The photos were taken at approximately 15m from the tunnel face. Roughly one-third of the photos were taken orthogonal to the tunnel face; the remaining two-third were taken at an oblique angle

Proceedings DOI: 10.21467/proceedings.133
ISBN: 978-81-957605-1-0

Series: AIJR Proceedings
ISSN: 2582-3922

approximately 45° to the tunnel face (in both directions). Each photo was taken at a different location, with at least 60% overlap with prior photo.

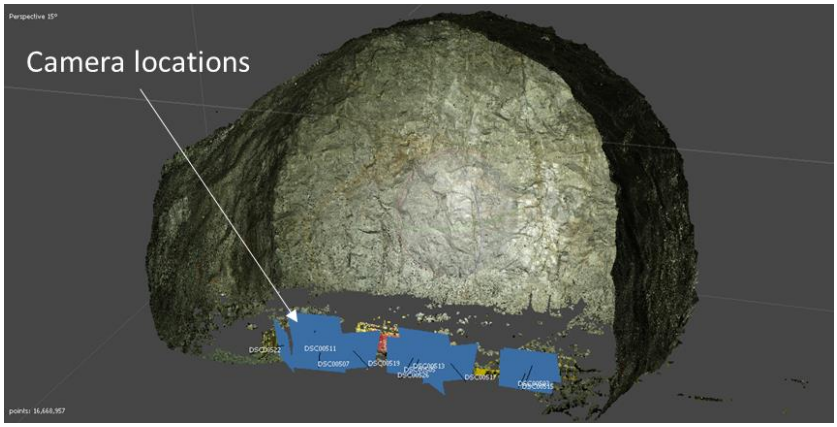

Figure 3: Camera locations and orientations for the 10 photos used for constructing the point cloud in Trial 2

A total of 58 and 39 photos were taken in Trial 1 and Trial 2 respectively. The 3D photogrammetry models were only generated by 10 selected photos in each trial, using the software Agisoft Metashape, which automatically generate point clouds from plain photos by SfM photogrammetry.

3.3 Data Processing

Initially, both the TLS- and SfM-derived point clouds were not orientated properly. In addition, the SfM-derived point clouds were not scaled properly. To correct the orientation and the scale, the point clouds were georeferenced using 5 to 7 ground control points (GCPs) sprayed by paint on two sides of the supported tunnel side walls (locations and close-up photo shown in Figure 4). As shown in the close-up screenshot in Figure 4, the GCPs can be easily identified on the colored point clouds. With real-world coordinates of the GCPs, the point clouds were georeferenced in the software CloudCompare (CloudCompare 2017). It is noted that a minimum of 3 GCPs are needed for georeferencing the point clouds and these should not be colinear.

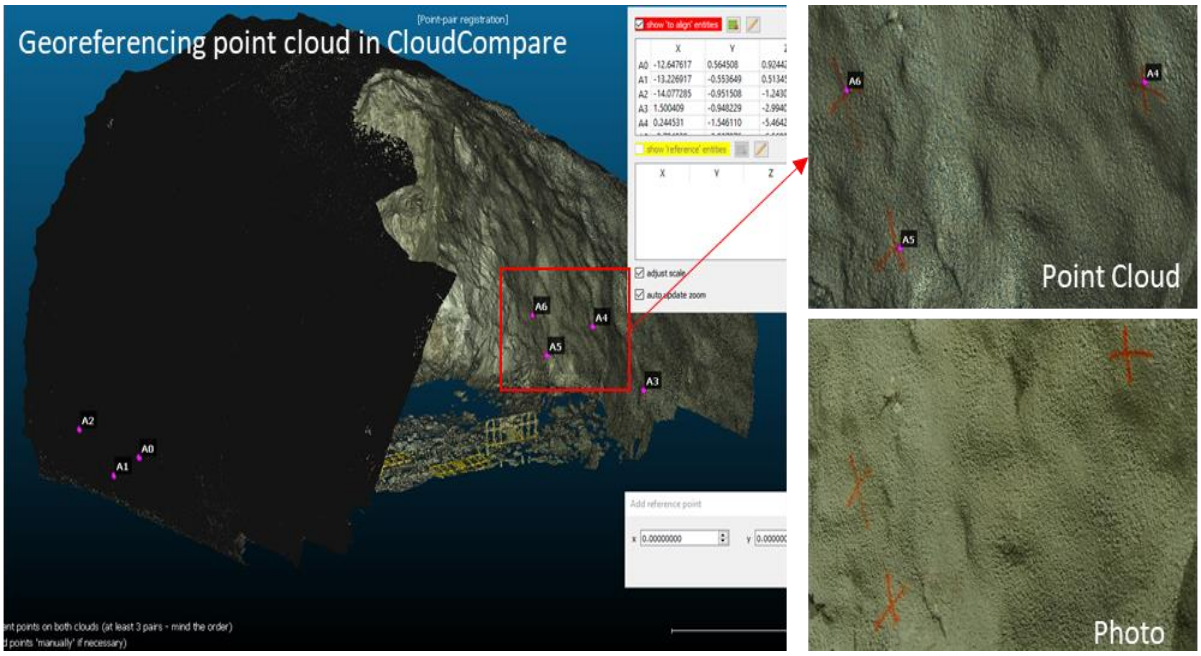

Figure 4: Ground control points – locations, close-up screenshot of the point cloud, and a photo for comparison

The point clouds are then further processed in CloudCompare to crop out the areas of interest, i.e., the tunnel face (Figure 5). The quality of the point clouds is further discussed in Section 5.1.

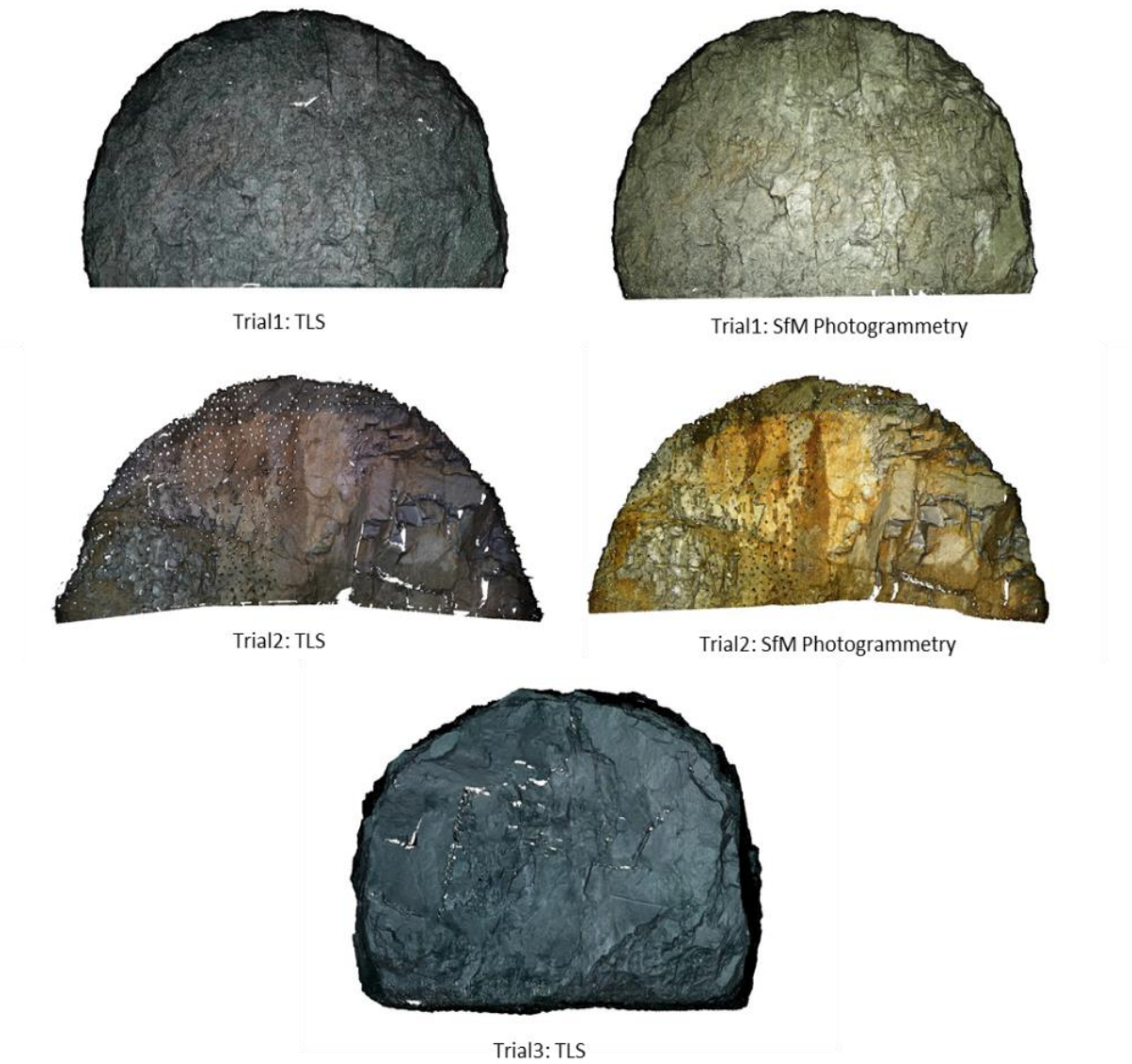

Figure 5: Point clouds of each tunnel faces in Trial 1 to Trial 3 after cleaning

4 Automatic Identification of Discontinuity Planes

4.1 Digital Rock Mapping with DRM2.0

Automatic identification of discontinuity planes was carried out with DRM2.0 developed by Aurecon Group (Gibbons et al. 2019) and FACETS (Dewez et al. 2016), a widely used plugin in CloudCompare. For comparison purpose, in all three trials, the TLS-derived point clouds were used, although as we will discuss in Section 6.1, the quality for SfM-derived point clouds are also sufficient for digital rock joint mapping.

DRM2.0 is integrated with the discontinuity analysis software DIPS developed by Rocscience. The extracted planes from DRM2.0 were analyzed in DIPS and subsequently classified into different joint sets. The classified results were then imported back to DRM2.0 and are shown with different colors for easy visualization (Figure 6). The spacing and persistence of each joint sets can also be computed, which will not be discussed in this paper. Interested readers can refer to Aurecon's submission on the

Proceedings DOI: 10.21467/proceedings.133
ISBN: 978-81-957605-1-0

Series: AIJR Proceedings
ISSN: 2582-3922

Benchmarking Exercise 2021 (CEDD 2021) and the presentation (Aurecon 2021) for a demonstration of DRM2.0's spacing and persistence function.

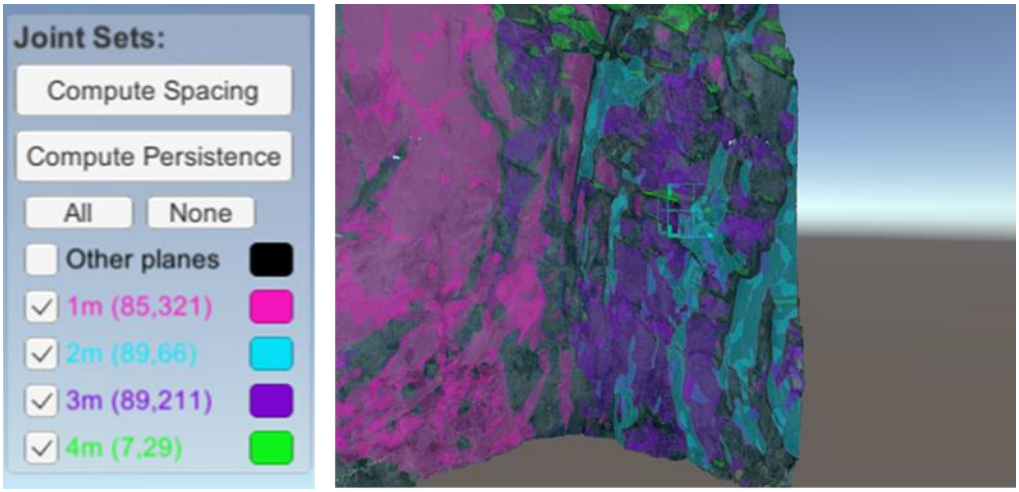

Figure 6: Functions in DRM2.0
(Left: Visualization of classified joint sets; Right: virtual scanline function using the sampling code)

DRM2.0 also contains a convenient "virtual scanline" function. The user can place a "cube" inside the 3D model with specified dimensions to sample extracted planes intersecting with the cube (Figure 6). In Trial 1 to Trial 3, a virtual scanline of 1m × 1m × 1m were used. RQD (rock quality designation), one of the six parameters in Q-value (NGI, 2015), were estimated based on planes intersecting the cube along three different axes. The locations of the scanlines used in each trial are shown in Figure **7**.

FACETS was also used on the same data, in addition to DRM2.0, to explore the application of automatic extraction of discontinuities for tunnel mapping.

4.2 Results

In general, the performance of the discontinuity extraction increases from Trial 1 to Trial 3. The results of the discontinuity extraction and the contoured stereoplots (plotted in DIPS) are shown in Figure **7**. A summary of the results is provided in Table 2.

Table 2: Results of automatic identification of discontinuity planes

Trial #	Planes identified		Major joint sets from DRM2.0 (Dip / Dip Direction)				Estimated RQD from DRM2.0
	DRM2.0	FACETS	J1	J2	J3	J4	
Trial 1	954	1707	(not classified)				91-96
Trial 2	1785	1707	86°/244°	84°/262°	48°/062°	-	73-97
Trial 3	2389	2362	85°/321°	89°/066°	87°/211°	07°/029°	55-72

Overall, both software identified similar discontinuity patterns in the three trials, except the density of the discontinuity sets may differ. For Trial 1, as shown in the Stereoplot in Figure **7**, the planes identified in DRM are predominantly subparallel to the tunnel face. A small proportion are along the tunnel side wall and crown. Closer inspection reveals that a lot of these identified planes are induced fracture surfaces (caused by blasting or breaking) instead of natural discontinuities. Since the identified natural discontinuities are masked by the fracture surfaces caused by the blasting or breaking works, joint sets were not classified in DRM for Trial 1. The results in FACETS for Trial 1 are similar, where blast/breaking-induced fracture surfaces dominate the extracted planes. The results are expected as the tunnel face in Trial 1 is massive with visually limited exposed discontinuity surfaces.

For Trial 2 and Trial 3, three to four joint sets could be classified based on the Stereoplot in both DRM and FACETS. The results are expected as the tunnel faces in Trial 2 and Trial 3 are blockier and with more exposed discontinuity surfaces than tunnel face in Trial 1.

The results show consistent increase of identified planes from Trial 1 to Trial 3, as the rockmass become blockier from Trial 1 to Trial 3. And the estimated RQD decreases accordingly.

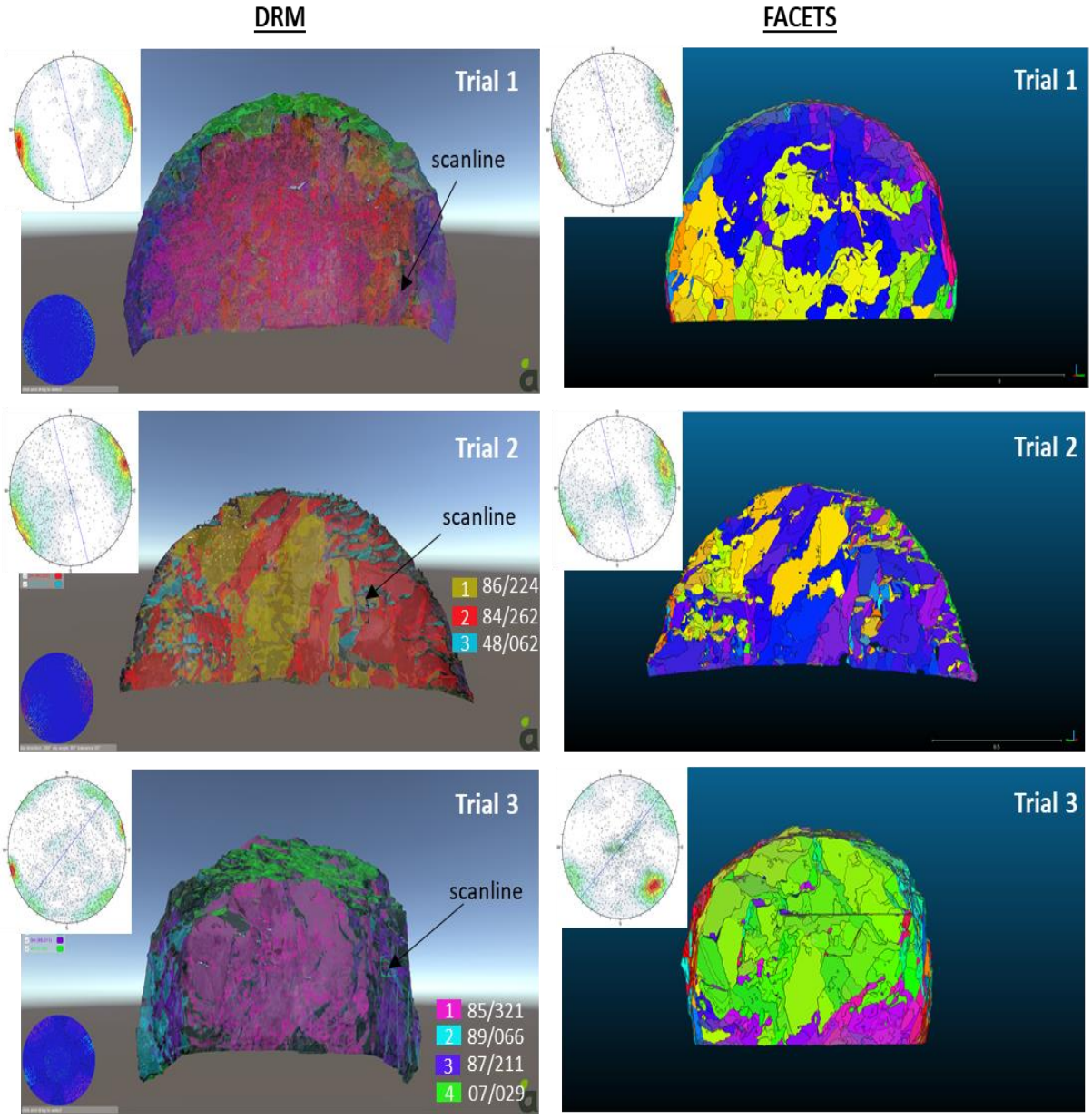

Figure 7: Results of the semi-automatic joint extraction

(Left column: results from DRM. Right column: results from FACETS as reference)

Another observation is that the reliability of the results could be affected by operational artifacts. Half of the tunnel face in Trial 2 was covered with split holes needed for drill and break excavation, where the internal profiles of which were picked up by the TLS. These were being shown as long 'spikes' behind the point cloud (Figure 8). Results show that the extraction of planes holding the split holes was unaffected in both software. However, FACETS identified a number of false planes associated with these split holes (Figure 8), which correspond to the plane cluster of approximately 45°/320° in the stereoplot. On the other hand, DRM2.0 was less affected (Figure 8).

Proceedings DOI: 10.21467/proceedings.133
ISBN: 978-81-957605-1-0

Series: AIJR Proceedings
ISSN: 2582-3922

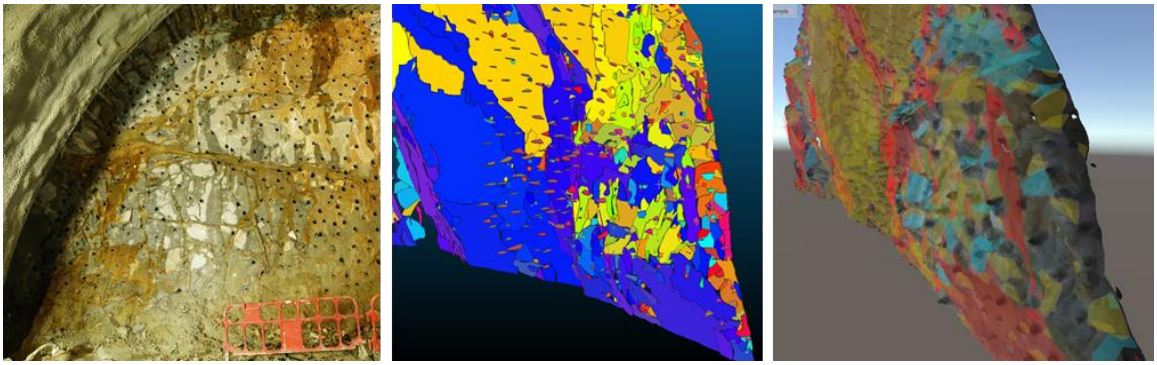

Figure 8: Effect of split holes on semi-automatic discontinuity extraction
(Left: Photo of the tunnel face in Trial 2 showing the split holes;
Middle: Automatic discontinuity extraction in FACETS;
Right: Automatic discontinuity extraction in DRM2.0)

In Section 5.2, we will further compare the results from digital rock mapping with the manual mapping records.

5 Comparisons and Verifications

5.1 Point Cloud Quality

One of the goals of this study is to evaluate the difference between acquisition methods on digital rock mapping in tunnels. We will compare the quality of point clouds from TLS and SfM photogrammetry and discuss the number of photos needed for SfM photogrammetry.

The accuracy of the point clouds was checked against the survey points on the excavation profiles measured using typical survey method with a total station. The accuracy is reported below as the RMS error of the differences between the point clouds and the 20 to 80 check points extracted from the corresponding 3D profile. The accuracy includes georeferencing errors.

5.1.1 TLS vs SfM Photogrammetry

In general, the quality of the SfM-derived point clouds (derived from 10 photos) is comparable to the TLS-derived point clouds, although the former has lower accuracies (Table 3).

As expected, the accuracy of the TLS-derived point clouds (4 – 10mm) are better than that of the SfM-derived point clouds (21 – 25mm) in both Trial 1 and Trial 2 but both are considered sufficient for rock joint mapping purpose as part of the tunnel excavation process. While the resolutions of the generated point clouds are dependent on the laser scanner settings or settings in the photogrammetry software, comparable resolution up to 4-5mm can be achieved.

Table 3: TLS VS SfM photogrammetry in Trial 1 and Trial 2

Trial #	Accuracy (mm)		Resolution (mm)	
	TLS	SfM-Photogrammetry	TLS	SfM-Photogrammetry
Trial 1	10	21	12 (medium-resolution scan)	5
Trial 2	4	25	5 (high-resolution scan)	4

In terms of occlusions, sub-horizontal discontinuities at higher elevations on the tunnel faces may be under-sampled as these may not be reached by the angle of incidence from the laser scanner, or the camera in the case of photogrammetry. An example of such sub-horizontal discontinuity is indicated in Figure 8 with a red arrow. In addition, occlusion can be from the lateral direction. Since the laser scans were taken at a further distance to the tunnel side walls, some of the discontinuities facing and

close to the tunnel side walls may be missed. An example is shown in Figure 9 by a yellow arrow. In contrast, SfM-derived point clouds miss fewer of these discontinuities as the camera stations are closer to the side walls.

In terms of visualization, SfM-derived point clouds have more vibrant colors, which can aid geologists to better visually identify possible features on the tunnel faces.

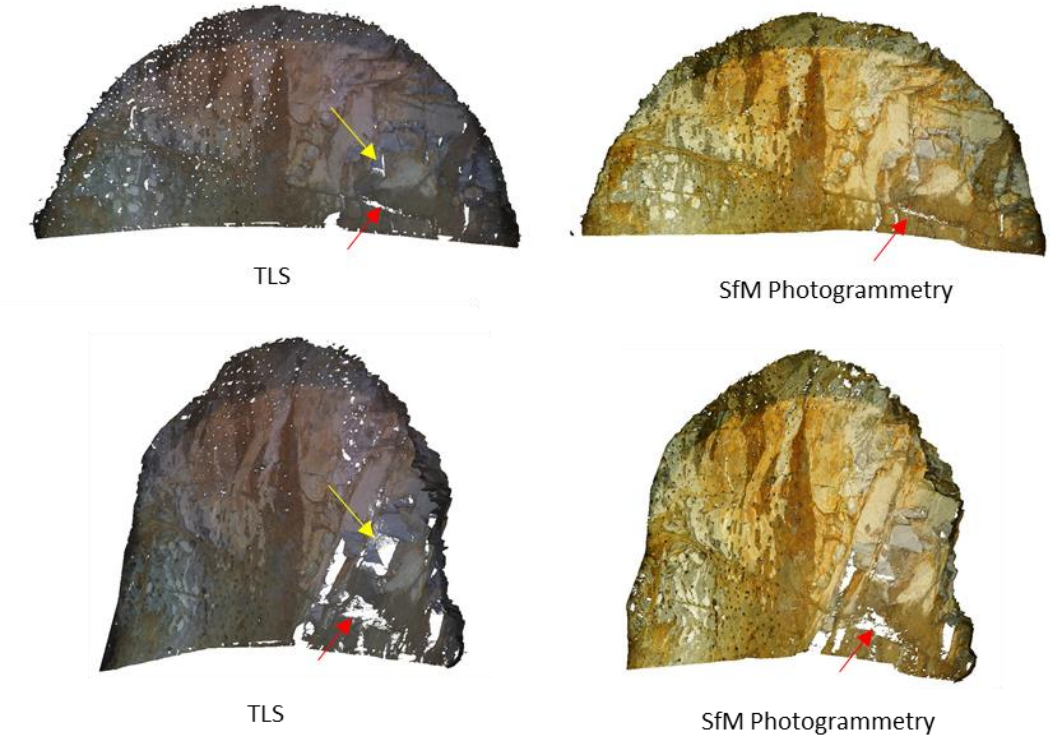

Figure 9: Occlusion in the point clouds produced by TLS and SfM photogrammetry

5.1.2 Number of Photos Required for SfM Photogrammetry

In Trial 1 and Trial 2, we found that when the number of photos used in SfM photogrammetry is reduced from over 30 to 10, the quality is more or less comparable.

Micheletti et al. (2015) suggested using 10 to 100 photos for 3D models at close scale (i.e., cm to 10s of m). They also pointed out that accuracy generally improves as more photos are used. However, as taking more photos also means longer surveying time in the tunnel, it is useful to know the minimum number of photos required to generate the same level of accuracy.

Garcia-Luna et al. (2019) has carried out systematic analysis on the effect of using different number of photos in SfM photogrammetry for tunnel mapping by Discontinuity Set Extractor (Riquelme et al. 2014), another popular software for automatic discontinuity extraction. Garcia-Luna et al. (2019) concludes that around 15 good quality photos are sufficient for a tunnel face with area of 50m^2.

We experimented with using only 10 photos to build the photogrammetry models. As indicated in Table 4, comparing to the models built from the maximum photos we took (i.e., 58 photos in Trial 1 and 39 photos in Trial 2), the accuracy of point clouds built from 10 photos are indeed lower. However, when the number of photos was reduced to 10, occlusion problem does not worsen significantly (Figure 10). The texture of the rock surfaces is also almost unaffected by reducing number of photos to 10 (Figure 11).

Proceedings DOI: 10.21467/proceedings.133
ISBN: 978-81-957605-1-0

Series: AIJR Proceedings
ISSN: 2582-3922

Table 4: Comparison of accuracy using different number of photos in Trial 1 and Trial 2

Trial #	Accuracy (mm)		Resolution (mm)	
	10 photos	58 photos (Trial 1) 39 photos (Trial 2)	10 photos	58 photos (Trial 1) 39 photos (Trial 2)
Trial 1	21	11	5	5
Trial 2	25	8	4	4

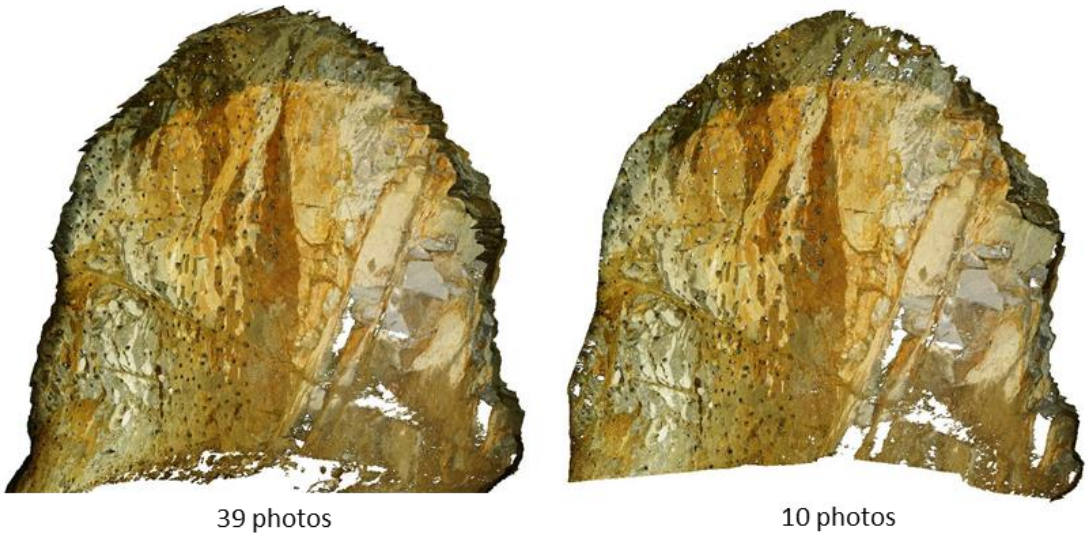

Figure 10: Occlusions in SfM-derived point clouds generated by different number of photos

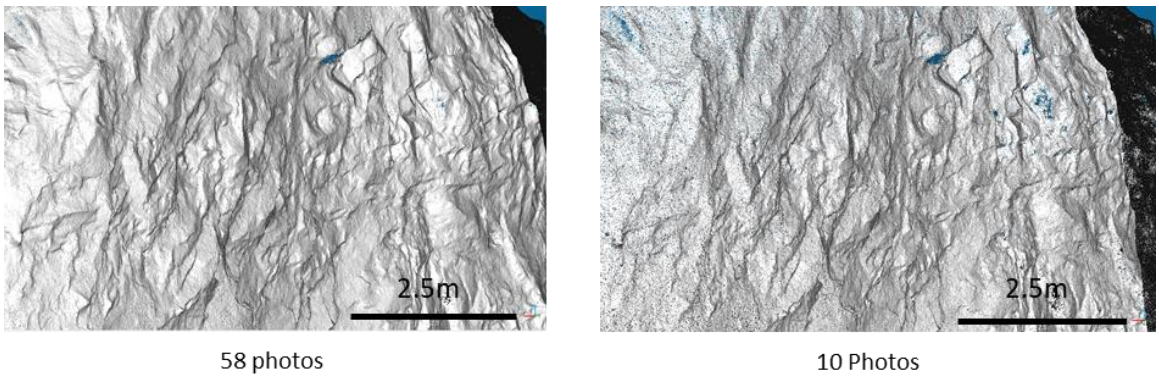

Figure 11: Textural comparison in the SfM-derived point clouds produced by different number of photos

5.2 Comparison with Manual Mapping

In general, the digital mapping results (Section 4.2) are found to be in good agreement with manual mapping in Trial 2 and 3, and to a lesser extent in Trial 1. However, the results also reveal limitations of current automatic discontinuity extraction techniques.

In the massive rock mass in Trial 1, while major joint sets cannot be effectively classified among the data with high noise ratio shown in the stereoplot (i.e., a large number of non-discontinuities being identified), the individual joint planes, especially the persistent ones, are still observed to be accurately extracted and their dip and dip directions are in line with the major joint sets in the manual mapping records. This is checked within DRM2.0, as DMR2.0 can display the orientation of the identified planes and the corresponding stereoplot location when the user clicks a plane on screen, providing a convenient and interactive experience.

Automatic discontinuity extraction in Trial 1 failed to identify two joint sets (i.e., 60-80°/340° and 15°/220°). The result is expected as these two sets have very limited areal exposure on the tunnel face.

Rather, these sets just appear as trace lines on the tunnel face. Same problem is also faced by FACETS (Figure **7**).

For the blockier rock mass in Trial 2, the subvertical joint sets J1 and J2 (86°/224° and 84°/262°) identified can only be roughly matched with the manual mapping record (80°/245-265° and 70°/280-320°). As these two sets are roughly subparallel to the tunnel face, they are also susceptible to being masked by noises created by the non-discontinuities. As a result, the spread of the clusters are large and the corresponding density peaks are not well defined.

In the blocky rock mass in Trial 3, the subvertical joint sets identified are in general rather close to the manual mapping record, with around 5° to 10° difference. Due to shallower dip angles, the moderately inclined to sub-horizontal joint sets are not identified with high certainty in Trial 2 (J3: 48°/062° vs 10-20°/100-130°) and Trial 3 (J4: 07°/029° vs 10-20°/050°).

Overall, the results are consistent in that as the rockmass becomes blockier from Trial 1 to Trial 3, the number of identified planes increases with increasing accuracy. In addition, while the range of the estimated RQD is large, it is in general consistent with manual mapping in all three trials (Figure 1 and Table 2).

6 Discussions

6.1 TLS vs SfM Photogrammetry for Tunnel Mapping

As discussed in Section 5.1.1, the quality of the SfM-derived point clouds is comparable to the TLS-derived point clouds. Considering the much cheaper cost of SfM photogrammetry (Table 5) and its ease of use, it is a good alternative to TLS (or even more preferable) when accuracy in the magnitude of 10^{-3}m is not required.

As for the data acquisition time, both methods are similar – less than half an hour (Table 5). Time needed for levelling the tripods for the TLS and for tuning the camera settings have been considered. As the data acquisition time is relatively short, these can be comfortably squeezed into the mapping / surveying time in the tunnel site schedule.

Back in office, data processing for data acquired with both methods (including processes such as scan registration, SfM photogrammetry, georeferencing and data cleaning) can be completed within an hour. Much of the time spent on the raw point cloud generation can be processed in background. Using DRM2.0, the digital rock mapping can be completed within 40 minutes.

Table 5: Comparison on cost and time for TLS and SfM photogrammetry

Data acquisition methods	Cost	Data Acquisition Time (Site)	Data Processing Time (Office)	Digital rock mapping with DRM2.0 (Office)
TLS	> 100,000 HKD (Scanner and accessories)	~24 minutes (2 high-resolution scans)	<1 hour	<10 minutes (calculation) + 30 minutes (interpretation and fine-tuning)
SfM photogrammetry	20,000 HKD (Camera + Lens + Agisoft Metashape)	~ 15 minutes (10 photos)	<1 hour (high accuracy settings)	

SfM photogrammetry has the additional advantages of being capable of producing point clouds with sharper colors, and less susceptible to occlusion problems from the sides. Therefore, from the authors' point of view, SfM photogrammetry is a preferrable data acquisition method for automatic

Proceedings DOI: 10.21467/proceedings.133
ISBN: 978-81-957605-1-0

Series: AIJR Proceedings
ISSN: 2582-3922

discontinuity identification for tunnel mapping based on the common tunnel excavation practice in Hong Kong.

The authors would highlight that some of the smart phones (e.g. iPhone 13 Pro) is incorporated with LiDAR scanner nowadays. A testing was carried out for the same tunnel face in Trial 2 using the LiDAR Scanner of iPhone 13 Pro. As shown in Figure 12, the quality of the 3D model is quite good and the details of the rock joint surface can also be seen. A key limitation for iPhone 13 Pro is the range of the LiDAR scanner – it is only up to 5m and therefore the tunnel face with a height of 12m could not be completely scanned in the testing.

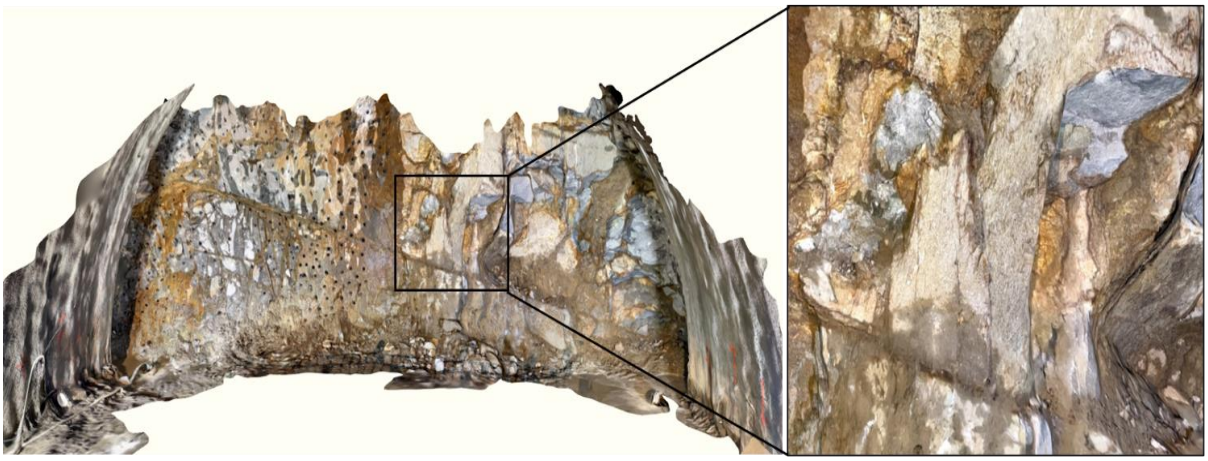

Figure 12: 3D model generated by iPhone 13 Pro for the tunnel face of Trial 2

6.2 Advantages of Digital Rock Mapping in Tunnels

Undoubtedly, digital rock mapping cannot replace manual tunnel mapping based on the current technology, and additional time and effort will be required if both digital and manual mapping have to be carried out (however it is considered achievable for both digital and manual mapping to carried out between the limited time of scaling and subsequent temporary support installation). Instead, digital rock mapping can supplement the traditional tunnel mapping work by providing much richer and more objective data.

In traditional tunnel mapping, the geologist can only observe the rock mass and measure the orientation of the discontinuities from a distance of tunnel face. And due to extreme time constraint, the geologist can only identify and record a small portion of all visible joints which he / she considers representative. Compare with rock slope mapping that can always afford much longer time for mapping, not many measurements of the discontinuities in tunnel mapping can be done and it is one of the reasons that only orientations of the major joint sets are recorded. The quality of the data collected is also highly dependent on the skill and experience levels of individual geologists. The mapping results are often not repeatable and reproducible for the same purpose.

In the case of digital mapping, if the point clouds are properly georeferenced, the dip and dip direction of individual discontinuity planes are, in theory, much more accurate and objective as the best-fit planes will be computed. Associated joint characteristics such as persistence can also be quickly and easily computed. Better data consistency can be maintained throughout the tunnel. In addition, in a blocky rock mass such as Trial 3, automatic extraction of discontinuity will be able to provide data on almost all the exposed joints, instead of only a few selected ones from traditional mapping. The RQD can also be estimated more objectively with a virtual scanline. With more robust statistics and more accurate data, a database of rock mass discrete fracture network (DFN) can be developed and hence more reliable and representable parameters of DFN can be developed in the detail design work (Figure 13). This database can definitely help the designer improve the underground support design. It is particularly useful for the extensive tunnels and caverns development in Hong Kong.

In digital rock mapping, a 3D record can be preserved for future use. The point clouds can be "revisited" in the future if needed, which improves quality control and cost saving. 3D records also communicate the findings better than using sketches, as 2D lines in rock mapping records often cause confusion. This makes it easier to communicate risks to client and stakeholders. This is particularly useful in tunnel and cavern construction involving scenarios with higher geometric complexity (e.g. tunnel/adit intersection and multiple stages / headings of excavation, especially for large span of excavation), and requiring more detailed record and study related to excavation profile (i.e. overbreak / underbreak) which could be affected by geological factors.

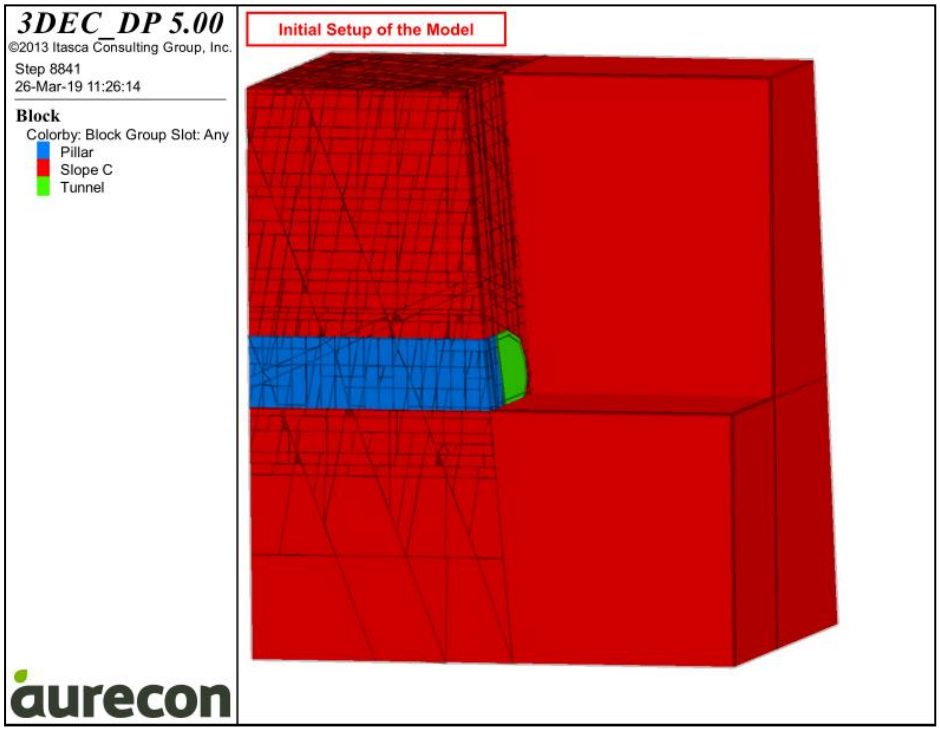

Figure 13: An example DFN developed for a rock tunnel support design

6.3 Limitations, Potential Solutions, and Further Investigations

While digital rock mapping in tunnel can supplement the traditional way to map tunnel face, there are various limitations to overcome. Some of the major limitations and possible solutions are listed below.

1) Trial 2 (Figure 9) shows occlusions on the tunnel face at several subvertical joints close to and facing the tunnel side walls, and also at several sub-horizontal joints at higher elevations. While the former type of occlusion is generally hard to avoid as it is impossible to get too close to the tunnel face beneath unsupported ground, the camera / laser scanner locations can be placed closer to the tunnel walls to alleviate the effect. For the latter type of occlusion, a possible way is to deploy unmanned aerial vehicles (UAV) in tunnels, as UAVs can take photos at higher elevation to cover the sub-horizontal joints. However, it is expected that the occlusion effect become less significant for smaller tunnels (e.g., water-carrying or drainage tunnels of smaller typical cross-section) as the tunnel size becomes smaller.
2) It is challenging for semi-automatic discontinuity extraction software (even for experienced geologists) to distinguish fractures formed by blasting or breaking from discontinuities. This is particularly relevant if the rockmass is massive (like Trial 1) where the automatically extracted planes may be masked by a large number of non-discontinuities (fractures and rock surfaces). At the current stage, for massive rock mass, or when only a few protruding rock joints are present, the best way is to just check the orientation of selected discontinuities by virtual manual measurements using software like the qCompass in CloudCompare.

Proceedings DOI: 10.21467/proceedings.133
ISBN: 978-81-957605-1-0

Series: AIJR Proceedings
ISSN: 2582-3922

3) Discontinuity traces cannot be extracted (i.e. discontinuity without a protruding surface but rather appear as a "line" on the rock surfaces). This may lead to a whole joint set being missed out statistically. Currently, while automatic extraction of traces based on curvature or color is being actively researched (e.g. Umili et al. 2013; Guo et al. 2019; Zhang et al. 2020), it appears that no software is available for trace extraction yet, except the Trace Tool in CloudCompare (Thiele et al. 2017), which is a tool to aid manual digitization of traces. Our team is currently in active collaboration and research with other professionals in this industry to develop ways for trace and block extraction (Figure 14).

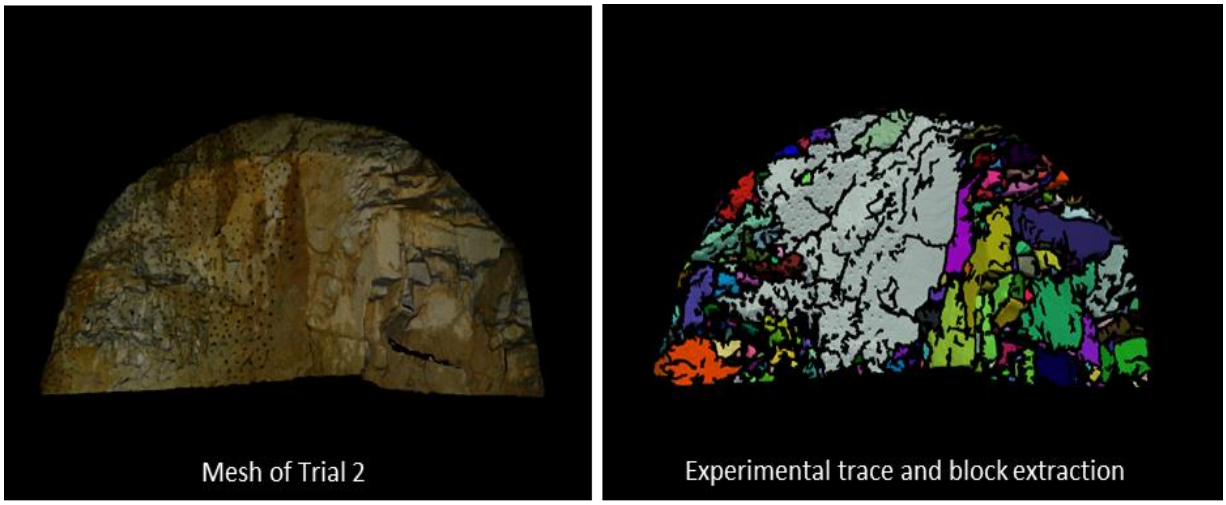

Figure 14: Experimental trace and block extraction (partial script developed by GeoRisk Solutions Ltd)

4) Some artifacts, such as the split holes in Figure 8, are difficult to clean. The results should be checked against actual field conditions and manually removed from digital results.
5) Roughness, alteration, infilling of the discontinuities cannot be reliably assessed from point clouds. These correspond to the Jr and Ja parameters in Q-value and control the discontinuity shear strengths. While there are not a lot of research on digital extraction of infilling and alteration, several attempts have been made on estimating the roughness, such as by calculating discontinuity roughness angle at different scales (Gigli and Casagli 2011), or correlating the RMS of the discontinuity profile to the Joint Roughness Coefficient (JRC) (Li et al. 2019). These may become part of digital rock mapping workflow in the future.

6.4 Other Potential Uses

Other than rock mapping, other uses of point clouds in tunnels include checking shotcrete thickness by comparing the pre-shotcrete and the shotcreted 3D models (Fekete et al. 2009), automatic extraction of steel arches (Zhang et al. 2019), automatic identification of roof bolts (Singh et al. 2021) and generating smooth and continuous 3D tunnel profile for overbreak and underbreak study (instead of using typical method by linking the limited number of individual survey points taken for each chainage for generating 3D tunnel profile).

7 Conclusions

We carried out three site trials at two drill-and-blast tunnels with two data acquisition methods: TLS and SfM photogrammetry. We find that if a magnitude of 10^{-3}m level of accuracy is not required, the quality of the SfM-derived point clouds is comparable with, or even better than, the TLS-derived point clouds. We find that 10 photos are sufficient to produce point clouds with good quality by SfM. Given the much cheaper cost, SfM photogrammetry is more preferable for digital mapping in tunnel. We analyzed the point clouds using Aurecon's in-house developed software DRM and another free software

FACETS. Both results are in good agreement with traditional mapping in blocky rock mass but less so when the rock mass is massive where joints appeared as “lines” instead of planes on the tunnel face. While at this stage digital rock mapping may not be able to save time and replace human judgement in some mapping-related activities (e.g. identifying potentially unstable blocks that warrant spot bolting), the technique can supplement traditional mapping by providing massive objective and consistent data, help to build up useful DFN database for underground development, and by providing 3D records for better quality control, cost saving and communication. Although this technology cannot replace traditional tunnel mapping at the moment, it is being continuously refined.

8 Declarations

8.1 Acknowledgements

The authors would like to thank the support from Johnathan Hart of GeoRisk Solutions Limited to the development of the scripts used in the experimental trace and block extraction in the initial stage.

8.2 Publisher’s Note

AIJR remains neutral with regard to jurisdictional claims in published maps and institutional affiliations.

References

Aurecon Hong Kong Limited. 2021. Benchmarking Exercise on Digital Rock Mass Discontinuity Survey. https://hkss.cedd.gov.hk/InnoTech2021/materials/presentation/13%20BM4-(Aurecon).pdf

CEDD. 2021. Review of Benchmarking Exercise on Digital Rock Mass Discontinuity Survey 2020. Hong Kong.

CloudCompare 2017 CloudCompare (version 2.9). 2017. Retrieved from http://www.cloudcompare.org/

Chan, T.H, Woodmansey, P., Suen, H.Y., Lee, S.W., Henderson, T. 2019. Application of Digital Engineering to Geotechnical Tunnel Design, Proceedings of HKIE Geotechnical Division Annual Seminar 2019.

Dewez, T.J., Girardeau-Montaut, D., Allanic, C., & Rohmer, J. 2016. Facets: A CloudCompare Plugin To Extract Geological Planes From Unstructured 3d Point Clouds. Int. Arch. Photogramm. Remote Sens. Spatial Inf. Sci., XLI-B5: 799-804.

Fekete, S., Diederichs, M. and Lato, M., 2009. Geotechnical applications of Lidar scanning in tunnelling. RockEng. Diederichs and Grasselli, Toronto, pp.1-12.

Gibbons, C., Hoel, O., Lo, K.P., Chiu, S.L., Yan, K.W., Lau, C.F., 2019. On The Application Of UAVs For Rock Joint Mapping – A Case Study. In HKIE, Proceedings of HKIE Geotechnical Division Annual Seminar 2019.

Gigli, G., & Casagli, N. .2011. Semi-automatic extraction of rock mass structural data from high resolution LIDAR point clouds. International Journal of Rock Mechanics and Mining Sciences, 48(2), 187-198.

García-Luna, R., Senent, S., Jurado-Piña, R., & Jimenez, R. 2019. Structure from Motion photogrammetry to characterize underground rock masses: Experiences from two real tunnels. Tunnelling and underground space technology, 83, 262-273.

Guo, J., Liu, Y, Wu, L., Liu, S., Yang, T., Zhu, W. & Zhang, Z. "A geometry-and texture-based automatic discontinuity trace extraction method for rock mass point cloud." International Journal of Rock Mechanics and Mining Sciences 124 (2019): 104132.

Li, X, Chen, Z., Chen, J., and Zhu, H. 2019. Automatic characterization of rock mass discontinuities using 3D point clouds." Engineering Geology 259: 105131.

Micheletti, N., Chandler, J.H., Lane, S.N., 2015a. Structure from motion (SFM) photogrammetry. In: Clarke, L.E., Nield, J.M. (Eds.), Geomorphological Techniques (Online Edition). British Society for Geomorphology, London Chap. 2, Sec. 2.2. https://dspace.lboro.ac.uk/2134/17493.

NGI. 2015. Using the Q-system: Rock Mass Classification and Support Design (handbook). Norwegian Geotechnical Institute, Oslo.

Riquelme, A. J., Abellán, A., Tomás, R., & Jaboyedoff, M. 2014. A new approach for semi-automatic rock mass joints recognition from 3D point clouds. Computers & Geosciences, 68: 38-52.

Singh, S.K, Raval,S & Banerjee,B. 2021. A robust approach to identify roof bolts in 3D point cloud data captured from a mobile laser scanner. International Journal of Mining Science and Technology 31, no. 2: 303-312.

Thiele, S.T., Grose, L., Samsu, A., Micklethwaite, S, Vollgger, S.A. and Cruden A.R. 2017. Rapid, semi-automatic fracture and contact mapping for point clouds, images and geophysical data. Solid Earth 8, no. 6: 1241-1253.

Umili, G, Ferrero, A. & Einstein, H. H. 2013. A new method for automatic discontinuity traces sampling on rock mass 3D model." Computers & Geosciences 51: 182-192.

Wong, D., Chan, K., Millis, S., 2019. Digital Mapping of Discontinuities. In HKIE, Proceedings of HKIE Geotechnical Division Annual Seminar 2019.

Zhang, Wenting, Wenjie Qiu, Di Song, and Bin Xie. "Automatic tunnel steel arches extraction algorithm based on 3D LiDAR point cloud." Sensors 19, no. 18 (2019): 3972.

Zhang, Keshen, Wei Wu, Hehua Zhu, Lianyang Zhang, Xiaojun Li, and Hong Zhang. "A modified method of discontinuity trace mapping using three-dimensional point clouds of rock mass surfaces." Journal of Rock Mechanics and Geotechnical Engineering 12, no. 3 (2020): 571-586.